Petrographic and chemical variation among the EH3 chondrites. M. Komatsu[1], T. J. Fagan[1], N. Ozaki[1], T. Mikouchi[2], and M. Miyamoto[2]. [1]Waseda University, 1-6-1 Nishiwaseda, Shinjuku, Tokyo 169-8959 (m.komatsu3@kurenai.waseda.jp), [2]Department of Earth and Planetary Science, University of Tokyo.

Introduction: Enstatite chondrites represent initial formation and metamorphism under highly reduced conditions. Like the other chondrite groups, the enstatite chondrites underwent various degrees of thermal metamorphism resulting in distinct petrologic types [1]. However, the petrologic types of enstatite chondrites are not always consistent with the geothermometry or mineral chemistory, indicating that enstatite chondrites underwent complex thermal histories [2].

Type 3 chondrites are the least metamorphosed type among chondrite groups. For ordinary chondrites, Sears et al. [3] subdivided type 3 into ten finer divisions (type 3.0 through 3.9) using thermoluminescence (TL) sensitivity as an indicator of metamorphic grade. Subsequently, some mineralogical changes with increasing subtype have been identified [4]. An approach similar to that of [4] has been applied to EH3 chondrites [5]; however, a systematic understanding of metamorphic reactions has not been attained and metamorphic sub-types have not been established for EH3 chondrites. In this study, we studied 5 EH3 chondrites in order to assess variations in texture and mineral compositions among the EH3 chondrites. We also compared these observations with EH4 and 5 samples to gain a broad perspective of metamorphism of EH chondrites.

Methods: We investigated polished thin section of ALHA81189, ALH84170, Sahara 97096, Y-691, and PCA82518 EH3 chondrites. Elemental maps collected by electron microprobe (JEOL JXA-8900 at Waseda University) were combined with petrographic microscope observations. Elemental X-ray maps were combined as false-color images and used as "base maps" for quantitative electron microprobe analyses of olivine and pyroxene and troilite on grid patterns. On the order of 90 to 200 analyses of each mineral were collected from each sample. Backscatterd electron images were obtained using a Hitachi S-3400 SEM at Waseda University and Hitachi S-4500 SEM at University of Tokyo. We also observed textures and collected mineral compositions in Indarch (EH4), St. Marks (EH5) and LEW 88180 (EH5).

Results:

All of EH3 chondrites in this study are dominantly composed if FeO-poor pyroxene. Metal and sulfide occurs as complex nodules which are composed of combinations of troilite, Fe-Ni metal, perryite, niningerite, djerfisherite, and daubreelite. Occasionally, oldhamite is also present.

Chondrule occurrence

ALHA81189 contains well-defined chondrules and chondrule fragments. Many chondrules are rimmed by silica or silica-rich rims in ALHA81189 and Y-691, whereas silica or silica-rich rims are not as abundant in ALH84170 and Sahara97096. In PCA82518, silica-rich rims were not identified. Instead, euhedral silica is observed inside chondrules (Fig. 1).

Sulfide nodules

Sulfide nodules are abundant in all EH3s. Sulfide/metal nodules in ALHA81189, ALH 84170 and Y-691 have sizes and shapes similar to silicate chondrules and are composed of combinations of troilite, kamacite, daubreelite, and niningerite. Generally, troilite and daubreelite occupy the cores of the spherules whereas kamacite usually occurs in the outer portions. Sulfides are more dispersed in PCA82518; the core-rim structure as described above is absent. Mixed sulfide/metal nodules are rare, and sulfides tend to occur as dispersed crystals in Indarch (EH4), St. Marks (EH5) and LEW 88180 (EH5).

Chemical compositions of ol, px and troilite

The Fa content of olivine, Fs content of pyroxene, and Ti and Cr contents in troilite show wide ranges of composition in the EH3 chondrites. Chemical compositions of troilite are shown in Fig. 2. It seems that Ti concentration in ALHA81189 is lower than the other EH3s and those in PCA is the highest.

Matrix mineralogy

EH3s contain matrix material which consist of fine-grained silicate crystals, small chondrule fragments and opaque materials filling the interstices between chondrules and chondrule fragments, as identified in [6]. This kind of matrix is also characterized as “clastic matrix” in [7]. This type of matrix is observed in ALHA81189, Y-691, ALH84170, and Sahara 97096.. The matrix of PCA82518 is distinct. It has a vein-like texture, is relatively bright in BSE, and includes bulbous kamacite crystals (Fig. 4e). Elongate enstatite crystals extending from chondrules into matrix are evidence of recrystallization in PCA 82518.

Discussion:

It is important to characterize the lowest end of the metamorphic sequence because type 3 chondrites should represent primitive material and the first stage of asteroidal metamorphism. Based on the textural characteristics of EH3 chondrites, we can subdivide EH3s into 3 distinct groups: (1) Primitive, ALHA81189 and Y-691; (2) low degree of

metamorphism, ALH84170 and Sahara 97096; moderately metamorphosed, PCA82518.

This trend is supported by the chemical composition of pyroxene and troilite compositions; primitive EH3s have high Fs content in pyroxene and low Ti content in troilite wheras metamorphosed EH3 has lower Fs content and higher Ti content in troilite. It suggest that the reduction (lower $f(O_2)$) during the thermal metarmorphism as suggested in [8].

In our study, it is shown that moderately metamorphosed EH3 has lower content of Cr in olivine than primitive EH3. This is consistent with the results from Bendersky et al. [5], suggesting the Cr redistribution from olivine into metal and sulfide phases during the thermal metamorphism of EH3 chondrites. The rounded shapes of Fe,Ni metal and sulfides in matrix in PCA 82518 and the elongate pyroxene crystals extending into the matrix and metal nodules may have resulted from a shock event. Some of the difficulties of unraveling metamorphic processes of the EH chondrites probably result from mixed effects of nebular reactions, thermal metamorphism and shock.

References: [1] Van Schmus W. R. and Wood J. A. (1969) *Geochim. Cosmochim. Acta*, 31, 747-765. [2] Zhang et al. (1995) JGR, 100, E5, 9417-9438. [3] Sears et al. (1983) *LPS XIV,* 682-683. [4] Grossman J. N. and Brearley A. J. (2005) *Meteoritics & Planet. Sci., 40,* 87-122. [5] Bendersky et al. (2007) L*PS, XXXVIII*, 2077. [6] Kimura et al. (1988) *Proc. Of the NIPR symp. On Antar.Meteor., 1,* 51-64. [7] Rubin A. E. et al. (2009) *Meteoritics & Planet. Sci., 44,* 589-601. [8] Fagan T. J. et al. (2010) *LPS XXVII,* 1534.

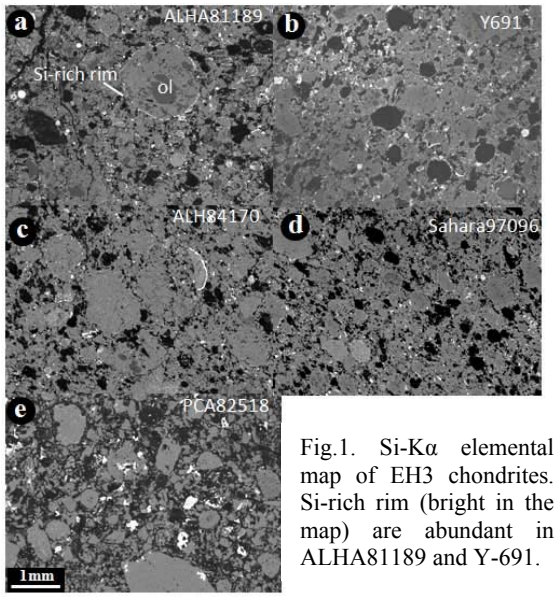

Fig.1. Si-Kα elemental map of EH3 chondrites. Si-rich rim (bright in the map) are abundant in ALHA81189 and Y-691.

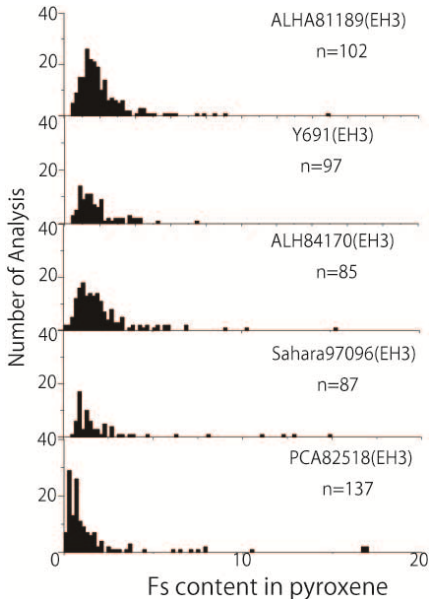

Fig.2. Histogram of Fs content (mol %) in pyroxene from EH3 chondrites.

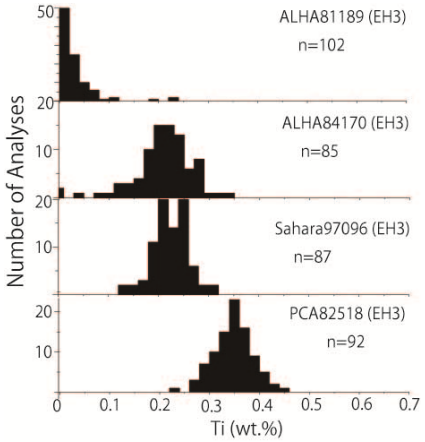

Fig.3. Histogram of Ti content (wt.%) in troilite from EH3 chondrites.

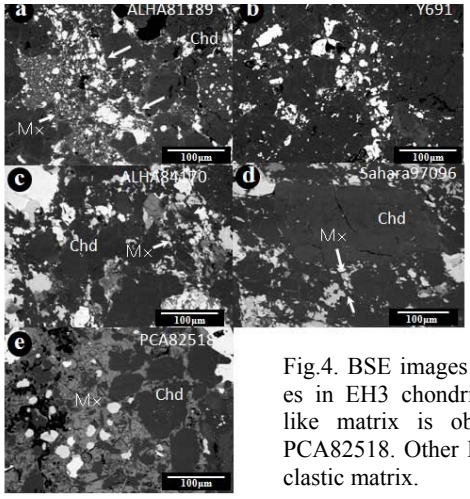

Fig.4. BSE images of matrices in EH3 chondrites. Vein-like matrix is observed in PCA82518. Other EH3s have clastic matrix.